Title
Serotonergic paraneurones in the female mouse urethral epithelium and their potential role in peripheral sensory information processing

Journal
Acta Physiologica, 222(2)

ISSN
1748-1708

Authors
Kullmann, FA
Chang, HH
Gauthier, C
et al.

Publication Date
2018-02-01

DOI
10.1111/apha.12919

Peer reviewed

HHS Public Access

Author manuscript

Acta Physiol (Oxf). Author manuscript; available in PMC 2018 May 22.

Published in final edited form as:

Acta Physiol (Oxf). 2018 February ; 222(2): . doi:10.1111/apha.12919.

Serotonergic paraneurones in the female mouse urethral epithelium and their potential role in peripheral sensory information processing

F. A. Kullmann[1], **H. H. Chang**[2], **C. Gauthier**[3], **B. M. McDonnell**[1], **J.-C. Yeh**[2], **D. R. Clayton**[1], **A. J. Kanai**[1,4], **W. C. de Groat**[4], **G. L. Apodaca**[1,5], and **L. A. Birder**[1,4]

[1]Department of Medicine, University of Pittsburgh School of Medicine, Pittsburgh, PA, USA

[2]Department of Urology, University of Southern California, Los Angeles, CA, USA

[3]Department of Biological Sciences, University of Pittsburgh, Pittsburgh, PA, USA

[4]Department of Pharmacology and Chemical Biology, University of Pittsburgh School of Medicine, Pittsburgh, PA, USA

[5]Department of Cell Biology, University of Pittsburgh School of Medicine, Pittsburgh, PA, USA

Abstract

Aim—The mechanisms underlying detection and transmission of sensory signals arising from visceral organs, such as the urethra, are poorly understood. Recently, specialized ACh-expressing cells embedded in the urethral epithelium have been proposed as chemosensory sentinels for detection of bacterial infection. Here, we examined the morphology and potential role in sensory signalling of a different class of specialized cells that express serotonin (5-HT), termed paraneurones.

Methods—Urethrae, dorsal root ganglia neurones and spinal cords were isolated from adult female mice and used for immunohistochemistry and calcium imaging. Visceromotor reflexes (VMRs) were recorded *in vivo*.

Results—We identified two morphologically distinct groups of 5-HT$^+$ cells with distinct regional locations: bipolar-like cells predominant in the mid-urethra and multipolar-like cells predominant in the proximal and distal urethra. Sensory nerve fibres positive for calcitonin gene-related peptide, substance P, and TRPV1 were found in close proximity to 5-HT$^+$ paraneurones. *In vitro* 5-HT (1 μM) stimulation of urethral primary afferent neurones, mimicking 5-HT release from paraneurones, elicited changes in the intracellular calcium concentration ($[Ca^{2+}]_i$) mediated by 5-HT_2 and 5-HT_3 receptors. Approximately 50% of 5-HT responding cells also responded to capsaicin with changes in the $[Ca^{2+}]_i$. *In vivo* intra-urethral 5-HT application increased VMRs induced by urethral distention and activated pERK in lumbosacral spinal cord neurones.

Correspondence: F. A. Kullmann, Department of Medicine/Renal and Electrolyte Division, University of Pittsburgh School of Medicine, Pittsburgh, PA 15261, USA. aurak@pitt.edu; aura240@yahoo.com.

Conflict of interests

The authors declare no competing financial interests.

Conclusion—These morphological and functional findings provide insights into a putative paraneurone-neural network within the urethra that utilizes 5-HT signalling, presumably from paraneurones, to modulate primary sensory pathways carrying nociceptive and non-nociceptive (mechano-sensitive) information to the central nervous system.

Keywords

calcium imaging; dorsal root ganglia; lower urinary tract; pERK; urethral sensations; visceromotor reflexes

Detection and transmission of peripheral sensory input to the central nervous system (CNS) are critical for proper organ function. Recent evidence highlights the importance of specialized non-neuronal sensory cells in the detection of peripheral stimuli. For example, in the skin, Merkel cells detect light-touch stimuli and directly synapse with sensory nerves to transmit this information to the CNS.[1] While the mechanisms underlying detection of peripheral somatosensory stimuli (such as touch or smell) are better understood, little is known about visceral stimuli.

The urethra is an organ traditionally viewed as a conduit for elimination of urine from the bladder. It is composed of an epithelium lining the lumen, lamina propria with a prominent vascular plexus, smooth muscle and an outer layer of striated muscle (called external urethral sphincter). The urethra functions in coordination with the bladder: it remains closed during bladder filling to maintain continence and it relaxes during voiding to allow flow of urine. These processes are controlled by parasympathetic, sympathetic and somatic innervation. Parasympathetic nerves release nitric oxide to relax the urethra during bladder voiding, while sympathetic nerves release noradrenaline to contract the urethra during bladder filling. The striated muscle receives somatic innervation that contracts the muscle ensuring continence during bladder filling. Afferent nerves providing input from the urethra consist of Aβ-, Aδ- and C-type fibres, and travel to the spinal cord via the pudendal, pelvic and hypogastric nerves.[2–6] The afferents travelling in the pelvic and pudendal nerves enter the spinal cord at the lumbosacral levels (L6-S1 in mice) and those travelling via the hypogastric nerve enter at the thoracolumbar levels (T13-L2 in mice).[2,3]

Urethral afferents potentially encode various stimuli including flow of urine, distention, changes in osmolarity or pH, and inflammatory mediators. Studies in humans and animals have shown that urethral afferent activity plays an important role in bladder function and visceral sensations including pain/nociception. Humans can feel urethral distention, passage of a catheter, or warm fluid into the urethra, as well as pain,[7–11] and it is reported that sensations of imminent micturition originate from the urethra and may be related to increase in intra-urethral pressure.[9] Efficient voiding also critically depends on input from the urethra. In human volunteers as well as in animals, stimulation of urethral afferents by flow, urethral distention, electrical stimulation of nerve fibres, chemical and mechanical intra-urethral infusion of various irritants (e.g. acetic acid, capsaicin, catheters) activates spinal cord neurones and triggers CNS-mediated urethral to bladder reflexes that elicit and/or augment bladder contractions and contribute to efficient bladder emptying.[2,7–10,12–20] Conversely, block of urethral afferent signals (e.g. using the Na^+ channel blocker, lidocaine)

abolishes bladder contractions elicited by urethral distention or flow and greatly impairs voiding.[7,8,16] Based on these experiments, it has been proposed that the bladder contraction during voiding is maintained by a positive urethra–vesical feedback elicited by the continued flow of urine through the urethra as well as urethral distention.[7,8] In pathologies, such as inflammation, it is believed that increased excitatory input from urethra contributes to pain as well as to bladder overactivity and symptoms of urgency and frequency.[21–25] For example, mechanical irritation of the rat urethra by catheter insertion[22] or placing latex strips into the urethra[23–25] produces a local neurogenic inflammatory response that involves capsaicin sensitive nerve fibres. Thus, there is clear evidence that stimuli that alter urethral afferent activity play an important role in bladder function, visceral sensations and pain/nociception. Yet, mechanisms underlying detection of urethral mechano- and/or chemosensory stimuli are not understood.

In the urethra, it may be expected that free nerve endings detect sensory stimuli; however, because the nerves may not reach the lumen where most sensory inputs originate, it is likely that stimuli are detected first by cells in the urethral epithelium, the cellular lining of the urethral lumen. The urethral epithelium is composed of several layers of cells forming an interface between the lumen and the underlying nervous, vasculature, connective and muscular tissues.[11] Besides epithelial cells, this epithelium contains other populations of cells, collectively called paraneurones (also named neuroendocrine, chemosensory or brush-like cells), identified by their transmitter content, including acetylcholine (ACh),[14] serotonin (5-HT)[14,26–33] or somatostatin.[32] Morphologically, some paraneurones are described as possessing dendrite-like processes spanning the epithelium, while others have an apical tuft of microvilli at the luminal surface of the urethra. The latter are also called ‘open’ paraneurones and are thought to respond to luminal stimuli.[29,34] Although these specialized cells were identified decades ago and are present in many species, including human, their functional properties and physiological roles are nearly unknown. A recent study[14] characterized a population of ACh^+ paraneurones, possessing apical microvilli, expressing taste receptors (TRPM5) and located in the proximity to presumed afferent nerve fibres expressing nicotinic cholinergic receptors. These paraneurones release ACh in response to bitter chemicals, such as those produced by infecting bacteria. Because intra-urethral infusion of bitter chemicals (e.g. denatonium) increases bladder activity, it was hypothesized that ACh^+ paraneurones act as ‘chemosensory sentinels’ to monitor the lumen for potential hazardous content.[14,35,36]

In this study, we characterize a distinct class of paraneurones which contain 5-HT and have an intimate anatomical relationship primarily with afferent nerves positive for calcitonin gene-related peptide (CGRP), substance P (SP) and TRPV1, suggesting that they serve sensory functions. Further, experiments mimicking the release of 5-HT from these cells demonstrate that 5-HT can activate urethral primary afferent neurones and associated spinal cord pathways. The results implicate urethral $5\text{-}HT^+$ paraneurones in the detection of physiological and possibly noxious peripheral stimuli.

Results

Differential distribution and morphology of 5-HT$^+$ cells in the urethra

Staining for 5-HT of female mouse, whole-mount urethra revealed 5-HT$^+$ cells embedded in the epithelium and distributed throughout the length of the urethra (Fig. 1a). There were no significant differences in the density of cells between the three regions of the urethra, proximal, mid and distal (Fig. 1b; $n = 4$ tissues; one-way ANOVA $F(2,9) = 2.732$, $P = 0.118$, followed by Tukey's multiple comparisons test among the three urethral regions; $P > 0.05$). However, there were significant differences in the morphology of 5-HT$^+$ cells along the urethral length. The majority of cells located in the mid-urethra had bipolar-like shapes, displaying elongated dendrite-like processes (Fig. 1c–d). The orientation of the processes was mostly circumferential around the lumen. Their total length, an estimated measure of epithelial span, ranged from ~66.5 to 252.2 μm, with an average of 164.5 ± 11 μm ($n = 23$ cells; Fig. 1g–i). Cells were also often positioned parallel to each other and some seemed to connect to each other (Fig. 1a). In contrast, the majority of cells located in the proximal and distal urethra had multipolar-like shapes, displaying several short dendrite-like processes with random orientations across the width of epithelium (Fig. 1e–f). The total length of processes ranged from ~40.3 to 175.9 μm, with an average of 116.5 ± 9 μm ($n = 20$ cells) for the proximal urethra and from ~42.2 to 165.6 μm, with an average of 103.5 ± 9 μm ($n = 18$ cells) for the distal urethra (Fig. 1g–i; data from 4 urethrae; one-way ANOVA, $F(2,58) = 10.67$, $P = 0.0001$; followed by Tukey's multiple comparisons test: P vs. M $P = 0.0028$ and D vs. M, $P = 0.0002$). Similar to previous studies in other species, these cells were confined within the epithelial layers, rarely penetrating into the subepithelial layer and were not found in the smooth muscle. Some cells displayed projections penetrating through the epithelium to the luminal surface (Fig. 2). The protrusions were usually at the intersection of large epithelial cells (inset in Fig. 2f). Regardless of morphology and location in the urethra, 5-HT$^+$ cells stained positively for the pan-neuronal marker PGP9.5, but not for the epithelial markers, cytokeratin 17 (CK17; Fig. 3) or CK5 (data not shown), suggesting a neuronal phenotype.

The urinary bladder contained very few 5-HT$^+$ cells which were randomly located (e.g. trigone, dome; ~2–7 cells/bladder; $n = 12$ bladders). No nerve fibre-like structures positive for 5-HT were observed in either the urethra or the bladder.

Relationship of 5-HT$^+$ cells with urethral nerves

To understand possible functions of the 5-HT$^+$ cells, we investigated their relationship with different classes of afferent and efferent nerve fibres (Fig. 4 and Table 1). Sensory afferent nerve fibres were identified by staining for neuropeptides: CGRP and SP. Presumed nociceptive C-fibre afferents were identified by staining for TRPV1. As there is overlap of markers, TRPV1$^+$ fibres are likely a subset of CGRP$^+$ and SP$^+$ fibres. Co-staining with 5-HT revealed that all 5-HT$^+$ cells were in close proximity (less than 3 μm) to these afferents (Fig. 4). In fact, CGRP fibres wrapped around the soma and dendrite-like processes of the 5-HT$^+$ cells with possible contacts (Fig. 4a–d). SP$^+$ and TRPV1$^+$ fibres were also located in close proximity to 5-HT$^+$ cells. While some of these fibres wrapped around 5-HT$^+$ processes, most ran along the dendritic processes and soma (Fig. 4e–l). The possibility of synaptic

connections between 5-HT$^+$ cells and nerve fibres was investigated by co-staining with synapsin I, a presynaptic marker believed to be involved in regulating the number of synaptic vesicles available for release.[37] All 5-HT$^+$ cells as well as the nerve fibres stained positively for synapsin I (Fig. 4m–o), suggesting that paraneurones have the machinery to release transmitters from synaptic vesicles and additionally, that communication with nerves could be bidirectional.

Sympathetic efferent nerves were identified by staining with tyrosine hydroxylase (TH) antibodies, and parasympathetic efferent nerves by staining with neuronal nitric oxide synthase (nNOS), and vesicular acetylcholine transporter (VAChT) antibodies. Qualitative observations indicated that these nerve fibres were present in the epithelium, albeit their density was much lower than that of the sensory fibres. Very rarely, 5-HT$^+$ cells in the mid-urethra were found in proximity to these nerve fibres but for most part, a close relationship between the 5-HT$^+$ cells and any of these efferent nerve fibres was not observed (Table 1). These results suggest that 5-HT$^+$ cells are likely to communicate almost exclusively with sensory fibres, including nociceptive TRPV1$^+$ fibres, supporting a potential role for paraneurones in afferent signalling.

5-HT activates urethral primary afferent neurones via 5-HT$_2$ and 5-HT$_3$ receptor subtypes

The close proximity of 5-HT$^+$ cells to sensory nerves suggests that release of 5-HT from paraneurones could activate these nerve fibres. Unidentified as well as cutaneous and striated muscle DRG neurones express several 5-HT receptor subtypes, including 5-HT$_2$ and 5-HT$_3$ receptors, and their activation increases neuronal excitability and contributes to nociception.[38–43] Thus, we investigated whether 5-HT can activate urethral primary afferent neurones identified by FAST DiI pre-labelling. 5-HT (1 μM) was applied to acutely dissociated L6 and S1 DRG neurones while imaging changes in $[Ca^{2+}]_i$ using fura-2AM (Fig. 5a). Approximately 80% of DiI-labelled and ~65% of non-DiI-labelled neurones responded to 5-HT with increase in $[Ca^{2+}]_i$ (Fig. 5b; Fisher's exact test, $P = 0.49$, indicates no significant differences between DiI and non-DiI populations in regard to responsiveness to 5-HT; cells from eight independent preparations from eight mice). Among the 5-HT responsive neurones, ~40–50%, of both DiI and non-DiI populations, also responded to capsaicin (0.5 μM) with increase in $[Ca^{2+}]_i$,, suggesting that they express TRPV1 and are likely nociceptive neurones (Fig. 5b). The magnitude of 5-HT-induced Ca^{2+} responses was similar in DiI and non-DiI populations (Fig. 5c; unpaired *t*-test $P = 0.49$) and was approximately one-third of the magnitude of capsaicin-induced Ca^{2+} responses. Although not quantified, spontaneous calcium oscillations were observed following exogenous application of 5-HT.

Repetitive applications of 5-HT (1 μM) at 15-min intervals produced responses that exhibited ~20% desensitization (not statistically different; Fig. 5d; DiI: paired *t*-test $P = 0.39$, $n = 9$ cells; non-DiI: paired *t*-test $P = 0.0539$, $n = 47$ cells). Among the seven 5-HT receptor subtypes, 5-HT$_3$ receptors are ion channels permeable to Ca^{2+} and 5-HT$_2$ receptors are metabotropic linked to the PLC-IP$_3$ pathway that can increase $[Ca^{2+}]_i$.[44] We next tested whether 5-HT$_2$ and 5-HT$_3$ receptors are involved in 5-HT-mediated increases in $[Ca^{2+}]_i$ in urethral afferent neurones. The non-selective 5-HT$_2$ receptor antagonist, ritanserin (1 μM), decreased the responses to 5-HT (1 μM), by ~40%, in both populations and reached

significance in the DiI population (Fig. 5e; DiI: paired *t*-test $P = 0.025$, $n = 7$ cells; non-DiI: paired *t*-test $P = 0.1073$, $n = 13$ cells). Similarly, the 5-HT_3 receptor antagonist, Y-25130 hydrochloride (1 μM), also decreased the responses to 5-HT (1 μM) by ~50%, and reached significance in the non-DiI population (Fig. 5f; DiI: paired *t*-test $P = 0.1862$, $n = 8$ cells; non-DiI: paired *t*-test $P = 0.0097$, $n = 25$ cells). While neither antagonist alone abolished the 5-HT-induced responses, when applied together, they significantly reduced them (from 28.1 ± 3.7 to 6.8 ± 1.7, $n = 11$ cells, two cells positive for DiI; paired *t*-test $P < 0.0001$). Together, these results indicate that multiple subtypes of 5-HT receptors are expressed in primary afferent neurones innervating the urethra as well as in other unidentified L6-S1 DRG neurones, and at least one population of capsaicin sensitive afferent neurones, presumably $TRPV1^+$, express 5-HT_2 and 5-HT_3 receptors.

Intra-urethral stimulation with 5-HT increases pERK in spinal cord neurones and sensitizes visceromotor reflexes (VMRs)

Painful stimulation such as noxious distention or irritation/inflammation of visceral organs (e.g. bladder/colon) results in visceral hyperalgesia and is positively correlated with increased neuronal pERK expression in regions of the dorsal horn receiving visceral sensory input.[45–49] To further investigate a potential role of peripheral urethral 5-HT signalling in nociception, we applied 5-HT intra-urethrally (1 μM; 15 min) and evaluated pERK activation in neurones located in the L6 segment of the spinal cord, which receives urethral afferent input. As a positive control, we used acetic acid (AA; 1%), a noxious stimulus that increases c-fos expression in the spinal cord after infusion into the urinary bladder, via activation of capsaicin sensitive nerve fibres (presumed $TRPV1^+$).[12] Regardless of treatment, few (between 0 and 3 cells per section; $n = 20$ mice) $pERK^+$ cells were detected in the L4 spinal cord sections, which do not receive visceral input. Similarly, a very low number of $pERK^+$ neurones (between 0–5 cells per section; $n = 2$ mice) was found in the L6 segments of mice that did not undergo any surgical or treatment manipulations. In animals receiving urethral infusion of saline (vehicle, $n = 6$ mice), $pERK^+$ neurones were observed in L6 segment in the dorsal horn areas receiving urethral afferent input (superficial dorsal horn) as well as in the sacral parasympathetic nucleus and dorsal commissure (Fig. 6a,e).[12,50,51] Stimulation with either 5-HT ($n = 9$ mice) or AA ($n = 5$ mice) significantly increased the number of $pERK^+$ neurones, compared to the number after saline infusion (Fig. 6b,c,e; one-way ANOVA $F(2,15) = 4.59$, $P = 0.027$, followed by Dunnett's multiple comparisons test between saline, 5-HT and AA; $P = 0.030$ and $P = 0.033$ respectively).

VMR is a spinobulbospinal reflex triggered by distention of visceral organs. It is used as a surrogate for visceral hyperalgesia in rodents because it is sensitive to analgesics and augmented by distention into nociceptive ranges as well as sensitization of afferents by inflammation/irritation.[52–55] To investigate whether peripheral 5-HT sensitizes afferent pathways activated by distention, we assessed the effect of intra-urethral 5-HT (1 μM) on VMRs during physiological intra-urethral distention (IUD) from 0 to 40 cmH_2O (Fig. 6f). We reason that during voiding, the urethra experiences pressures equal to bladder pressure necessary to expel urine, which in mice is ~30–50 cmH_2O.[56] Thus distention up to 40 cmH_2O is likely not noxious. Responses quantified as area under the curve (AUC) were compared between intra-urethral infusion of saline, 5-HT and the positive control, AA (1%).

In the saline group, graded distention of the urethra triggered VMR that did not significantly increase with increasing pressures, suggesting that nociceptive range had not been attained even at the highest pressure tested (40 cmH_2O). In contrast, in both 5-HT and AA groups, VMR increased proportionally with pressure. In the AA group, VMR-AUC was significantly increased compared to saline group at 30 cmH_2O and 40 cmH_2O during IUD (one-way ANOVA Kruskal–Wallis test $P = 0.026$, followed by Dunn's multiple comparisons; $P = 0.03$, $P = 0.02$ respectively). In the 5-HT groups, VMR-AUC was significantly increased compared to saline group at 40 cmH_2O during IUD (one-way ANOVA Kruskal–Wallis test $P = 0.013$ followed by Dunn's multiple comparisons; $P = 0.04$). Together, these results indicate that 5-HT and AA produced sensitization of pathways conveying mechano-stimuli, suggesting that peripheral 5-HT signalling can activate and perhaps sensitize mechano-sensitive afferent pathways.

Discussion

This study identified morphologically distinct nonepithelial 5-HT^+ cells, termed paraneurones, located in close proximity to sensory nerve fibres positive for CGRP, SP and TRPV1 and possessing the machinery (synapsin I) necessary for releasing transmitters. Experiments mimicking potential release of 5-HT from paraneurones and activation of afferent neurones indicated that 5-HT increases $[Ca^{2+}]_i$ in urethral primary afferent neurones via activation of 5-HT_2 and 5-HT_3 receptors, activates pERK in lumbosacral spinal cord neurones receiving input from the urethra and sensitizes responses to mechano-stimulation (distention) of the urethra. These results suggest that peripheral 5-HT signalling could be involved in transmission of sensory information from the urethra to the CNS. Because 5-HT is expressed solely within the urethral paraneurones, which are anatomically positioned to sense the epithelial environment and exhibit a close relationship to afferent nerves, it seems reasonable to propose that these paraneurones function as important detectors and transmitters in the urethral sensory mechanisms. The exact nature of the stimuli, specific ion channels/receptors used by paraneurones to detect stimuli and mechanisms involved in paraneurone-afferent communication remain to be further investigated.

Urethral 5-HT^+ cells morphology

Previous studies investigated 5-HT^+ cells in the urethra of different species using transverse sections.[26,27,29–33] It is now clear that this methodology underestimates the morphological complexity of these cells as well as their relationships with each other and with nerve fibres; these characteristics are better captured using whole-mount preparations and confocal microscopy. Using this methodology, two morphologically distinct 5-HT^+ cell types that were also located in distinct areas were observed in the female mouse urethra. Bipolar-like cells with elongated dendrite-like processes were predominant in the mid-urethra, while multipolar-like cells with shorter processes oriented in various directions were predominant in the proximal and distal urethra (Fig. 1). These cells were phenotypically distinct from epithelial cells, stained for a neuronal marker, and were not interstitial cell-like based on previous studies[57,58] that did not identify c-kit or vimentin-positive cells in the urethral epithelium. Cells with similar morphology were reported in the urethra of different species, such as human,[27,31] dog,[29] cat,[59] guinea-pig[28] or sheep,[32] although phenotype and distinct

anatomical location were not fully investigated. In the female mouse, urethra 5-HT$^+$ cells were distributed uniformly throughout the urethra (Fig. 1). In contrast, in the male rat, 5-HT$^+$ cells were densely distributed in the prostatic urethra, but sparsely distributed in the membranous and spongy parts of the urethra.[33] Together, these distinct morphological features and anatomical locations suggest that different classes of 5-HT$^+$ cells may detect different stimuli and likely serve different functions, which could differ based on sex. For example, bipolar cells with elongated dendrite-like processes which span a longer distance in the epithelium could be involved in sensing mechanical stimuli that may involve coordination across larger urethral areas (e.g. stimuli resulting from the urethral smooth muscle contraction/relaxation). Cells reaching the lumen may be involved in the detection of luminal stimuli such as flow, urine pH or osmolarity; cells that do not reach the lumen may be involved in sensing stimuli that affect deeper layers of the epithelium, including mechanical (e.g. distention, pressure/tension) or chemical (e.g. tissue acidosis) stimuli. The role of different subclasses of 5-HT$^+$ paraneurones remains to be further investigated.

Relationship with afferent nerves and functional implications

Previous ultrastructural studies reported that paraneurones contain electron-dense granules, indicative of vesicles storing 5-HT and possible other transmitters. [28,59,60] Our data showed that 5-HT$^+$ paraneurones stain positively for the presynaptic marker synapsin I, a protein involved in linking synaptic vesicles to the cytoskeleton and regulating the number of available vesicles for release[37] (Fig. 4). This suggests that these cells possess machinery needed for the release 5-HT. Once released, 5-HT can then act on neighbouring nerve fibres and/or epithelial cells (Fig. 7). It is unknown whether urethral epithelial cells express 5-HT receptors and whether their activation would release transmitters (such as ATP) that can activate the afferent nerves and/or the paraneurones. However, the afferent nerves express several types of 5-HT receptors [41] and in other systems, 5-HT depolarizes C and Aδ neurones,[40] modulates the excitability of visceral afferent C-fibres[39] and contributes to nociception by activating different receptors including the 5-HT$_3$ receptors.[42,43] Likewise, our experiments stimulating urethral afferent neurones *in vitro* indicated that a large percentage (~80%) of these neurones respond to 5-HT with increases in $[Ca^{2+}]_i$ mediated by 5-HT$_2$ and 5-HT$_3$ receptors (Fig. 5). Approximately half of the 5-HT responsive neurones were unresponsive to capsaicin, suggesting that 5-HT plays a role in sensory signals that may not be necessarily nociceptive. While we do not know the endogenous stimuli that activate urethral 5-HT$^+$ paraneurones, in the skin, Merkel cells, recently shown to be the light-touch mechano-detectors, are positive for 5-HT and synapse with the slowly adapting (SA1) low-threshold mechanoreceptor afferent fibres. Serotonin released during mechanical distortion of the Merkel cell membrane can activate 5-HT$_2$ and 5-HT$_3$ receptors on the SA1 fibres and alter action potential generation.[1,61–63] Similarly, it is possible that a subpopulation of urethral 5-HT$^+$ paraneurones may serve as mechano-detectors and release 5-HT, for example, in response to distention and/or pressure in the urethra. In support, VMR recordings indicated that intra-urethra 5-HT application during distention increased VMRs compared to saline application (Fig. 6f), suggesting that peripheral 5-HT can activate afferent pathways that convey mechanical stimuli. VMR is a spinobulbospinal reflex triggered by distention of visceral organs. VMR is traditionally considered a surrogate measure of nociception because it is sensitive to analgesics and it is augmented by distention

into noxious ranges and by sensitization of afferent nerves (e.g. by inflammation/irritation).[46,52–55] In our experiments, VMR was triggered by urethral distention to pressures up to 40 cmH_2O. These pressures are experienced by the urethra during voiding when urethral pressure is equal to bladder pressure necessary to expel urine, which in mice rises to ~30–50 cmH_2O,[56] thus not considered noxious. Accordingly, graded distention (0–40 cmH_2O) in the presence of saline did not increase VMR. However, the same distention in the presence of 5-HT or acetic acid significantly increased VMR (Fig. 6f), suggesting sensitization of these pathways. Together, these data suggest that peripheral 5-HT can stimulate and perhaps sensitize afferent pathways that convey mechanical stimuli from the urethra to the CNS.

The presence of $TRPV1^+$ fibres in close proximity to $5\text{-}HT^+$ cells (Fig. 4) and the demonstration that half of the urethral afferent neurone population responded to capsaicin and 5-HT (Fig. 5) suggest that peripheral 5-HT could also activate nociceptive pathways. In support, intra-urethral infusion of 5-HT activated pERK in the lumbosacral spinal cord neurones receiving input from the urethra (Fig. 6). The MAPK pathway and ERK1/2 phosphorylation have been implicated in initiation and maintenance of nociceptive behaviour (i.e. inhibitors of ERK 1/2 reduce pain) in various models of somatic and visceral pain;[45–49] thus, it is likely they may serve similar roles in the urethral pathways.

Alterations in 5-HT signalling play an important role in pathologies associated with pain in many systems. [64–66] They have been well documented in major gastrointestinal (GI) disorders such as inflammatory bowel disease, coeliac disease or irritable bowel syndrome and have been correlated with increased afferent signalling and pain sensitivity.[65–67] These alterations include changes in the number of $5\text{-}HT^+$ cells (known in the gut as enterochromaffin cells), increased 5-HT release or increased 5-HT availability due to decreased expression of the serotonin transporter – SERT.[65–67] Like in the GI, some of the common urethral pathologies such as urethritis, inflammatory polyps or cysts, strictures and in some cases the use of catheters are also characterized by pain, inflammation of the mucosa and/or neurogenic inflammation.[23,68–70] In rats, irritation of the urethra by mechanical stimulation due to catheter insertion induced neurogenic inflammation which was dependent on capsaicin sensitive nerves (i.e. systemic treatment with capsaicin to desensitize the nerves reduced the inflammation).[22,24,25] Our data showing that nerve fibres in close proximity to paraneurones stained positive for synapsin I suggest that the communication between nerves and paraneurones can be bidirectional (Fig. 7), whereas the nerves can release peptides (CGRP, SP, NKA) that act on paraneurones and influence 5-HT release. Neurogenic inflammation is typically associated with increased release of peptides from the afferent nerves, which triggers the release of 5-HT and other mediators from the affected tissue, increasing neuronal excitability and contributing to pain.[71] Thus, in urethral pathological conditions associated with neurogenic inflammation, this could result in a positive feedback loop between paraneurones and nerves that could contribute to inflammation and pain. In summary, in pathologies, it is conceivable that changes in the properties of urethral paraneurones could augment afferent nerve excitability and alter lower urinary tract function and visceral sensations, including pain. A better understanding of the properties of these cells may lead to identification of new targets for treating disorders associated with pathological conditions in the urethra.

Physiological significance—Peripheral visceral afferent signalling is crucial for proper function of organs. Sensory input from the urethra plays an important role in bladder function and visceral pain perception. However, the mechanisms underlying detection, processing and transmission of urethral sensory information are poorly understood. Our experiments identified 5-HT$^+$ paraneurones that are anatomically positioned to sample the urethral epithelial environment and transmit this information to adjacent nerves. Thus, this study provides an anatomical substrate for the existence of a urethral sensory network in which 5-HT$^+$ paraneurones may play a role as sensory detectors. Further studies are needed to determine the type of stimuli detected by 5-HT$^+$ paraneurones and mechanisms triggering transmitter release leading to activation and/or modulation of non-nociceptive and nociceptive afferent pathways under physiological and pathological conditions. Together with previous studies that proposed a role of ACh-expressing cells in the detection of bacterial infection, [14,35,36] our findings strongly support a role of different populations of specialized paraneurones (5-HT$^+$, ACh$^+$) in the detection, processing and transmission of different sensory modalities (e.g. mechano- and chemosensation) related to specific functions (e.g. distension, detection of flow or sensing bacterial infection in the urinary tract, nociception).

Materials and methods

All materials included in this paper conform with recommendations from ‘Good Publishing Practice in Physiology: Good publication practice in physiology.’[72]

Animals

Adult female mice C57BL/6J (5–8 weeks, 20–25 g; $n = 69$) were purchased from Jackson Laboratory (Bar Harbor, ME, USA). This study was performed in females only due to the large anatomical differences between male and female urethra. In the male, the urethra is comprised of three main segments prostatic, membranous and spongy (penile). Previous studies in other species (e.g. rat, dog, human, sheep)[29,31–33] have shown the expression of serotonergic paraneurones in the male urethra. However, the distribution and density of these cells across different parts of the urethra may differ from female and also may differ across species; [29,33] thus, 5-HT paraneurones in male mouse urethra will be investigated in a future study. All procedures were approved by the Institutional Animal Care and Use Committee at the University of Pittsburgh, which adheres to NIH Guidelines for the Care and Use of Laboratory Animals. The University of Pittsburgh is accredited by the Association for Assessment and Accreditation of Laboratory Animal Care (AAA-LAC). Mice were housed under controlled conditions (20 ± 1 °C and humidity 30–70%), four to five per cage on a 12-h light–dark cycle, and fed with standard chow. After surgical procedures, mice were single-housed with enhanced enrichment.

Drugs

5-HT and capsaicin were purchased from Sigma-Aldrich (St. Louis, MI, USA). The 5-HT$_2$ receptor antagonist, ritanserin, and the 5-HT$_3$ receptor antagonist, Y-25130 hydrochloride, were purchased from Tocris Bioscience. Concentrations of chemicals used in this study were based on reported IC$_{50}$ of antagonists and previous studies.[39] All drugs except for capsaicin

were dissolved in water to prepare 1 or 10 mM stock solutions. Capsaicin was diluted in DMSO to 10 mM stock solution. All drugs underwent further dilutions in the bath solution. Final DMSO concentration was < 0.01%.

Tissue collection and preparation for immunohistochemistry

Bladder, urethra and spinal cord segments (L4, L6 and S1) were collected from deeply anesthetized mice (5% isoflurane in O_2) perfused with phosphate-buffered saline (PBS) and 4% paraformaldehyde (PFA). Tissue was postfixed for 2–4 h in 4% PFA, immersed in 30% sucrose for 24–48 h, embedded in optimum cutting temperature compound (Tissue-Tek OCT, Sakura Finetek, Torrance, CA, USA) and cut at 8–20 μm thickness. For the urethra whole-mount staining experiments, tissue was collected from mice perfused only with PBS. Urethrae were dissected out, cut open, pinned down flat and postfixed in 4% PFA for 1–2 h. Tissues were washed with PBS, incubated with permeabilizing/blocking solution (0.5% Triton X-100 and 10% donkey or goat serum), followed by the primary antibody (24 h at 4 °C) and secondary antibodies (Alexa Fluor 488 or 555; 1 : 1000; 2 h at room temperature; Life Technologies, Carlsbad, CA, USA). Table 2 summarizes primary antibodies used in this study. Nuclei were counterstained with DAPI (4′,6-diamidino-2-phenylindole, 1 : 2500, Thermo Fisher Scientific Corporation, Pittsburgh, PA, USA) or TOPRO-3 Iodide (TOPRO; 1 : 1000; Thermo Fisher Scientific Corporation) added with the secondary antibodies. Some tissues were counterstained with phalloidin, a stain for F-actin filaments, conjugated with rhodamine or FITC (1 : 1000; Thermo Fisher Scientific Corporation) to label the epithelium. The slides were mounted in medium ProLong Gold Antifade Reagent (Thermo Fisher Scientific Corporation). Control experiments were performed by omitting the primary antibody.

Confocal microscopy and image processing

Images consisting of single optical sections were taken with a Leica DM6000B upright fluorescent microscope equipped with 5× 0.15NA air objectives using VOLOCITY 4D software (Perkin Elmer, Waltham, MA, USA) or a BX-62 Olympus upright fluorescent microscope equipped with 10× 0.4NA and 20× 0.7NA air objectives using HCIMAGE software (Hamamatsu Photonics, Bridgewater, NJ, USA). Confocal imaging was performed using an inverted confocal Leica TCS SP5 CW-STED microscope equipped with an HCX PL APO 63× 1.3NA glycerol objective and the appropriate lasers. The photomultipliers were set at 600–1200 V, and 8-bit images were collected using 4–8 line averages combined with 4–8 frame averages. Serial 0.13, 0.25 or 0.5 μm Z-sections were acquired and images imported into VOLOCITY 4D software or IMAGEJ (National Institutes of Health, Bethesda, MD, USA) for image reconstruction and quantification. Images presented here are single optical sections, maximum projections of Z-stacks (projected by maximal fluorescence intensity) or 3D reconstructions of Z-stacks assembled using VOLOCITY 4D software.

Quantification of 5-HT$^+$ cells and length of cell processes

The whole-mount urethral tissue was divided into three parts: proximal (P), middle (M) and distal (D), relative to the bladder neck. The width and length of each part of the urethra were ~2.5–3 mm (Fig. 1). Digital pictures were acquired with 20× 0.7NA air objectives and imported into IMAGEJ. A threshold function (based on preparations without the primary

antibody) was applied such that all 5-HT$^+$ cells were visible. A 200 × 200 μm grid was laid over the pictures, and cells were counted in each region of the urethra. Results from four urethrae were averaged and expressed as number of cells per tissue area. For the total length of cell processes, images of projected Z-stacks (0.25 μm step) were imported into IMAGEJ. Using the built-in function 'Simple Neurite Tracer,' cells were traced as illustrated in Figure 1h,i and the total length of processes calculated and exported into excel. Results were averaged from 18 to 23 cells per urethral region from four mice.

Urethra stimulation for assessment of phosphorylated extracellular signal-regulated kinases (pERK) in the spinal cord

ERK is a member of the mitogen-activated protein kinase (MAPK) superfamily. Acute noxious peripheral stimuli, such as capsaicin, acetic acid and inflammation, activate primary afferent nerves and induce phosphorylation of ERK in neurones in the spinal cord areas receiving primary afferent input.[45–49] In these experiments, we used pERK assessment to determine whether peripheral stimulation of the urethra with 5-HT (mimicking 5-HT release from paraneurones), activates spinal cord pathways. Under urethane anaesthesia (1.5 mg kg $^{-1}$, i.p., Sigma-Aldrich; n = 22 mice), a laparotomy was performed and the bladder cut open at the dome. A PE50 catheter was inserted and advanced into the urethra, approx. 2 mm from the bladder neck and secured with a 5.0 suture (schematic in Fig. 6d). Urethra was perfused with either saline (0.9% NaCl; n = 6 mice), acetic acid (AA, 1%; n = 5 mice) or 5-HT (1 μM; n = 9 mice) for 15 min at a rate of 0.1 mL min^{-1} using a syringe pump. The mice were then perfused with PBS followed by 4% PFA, and lumbosacral spinal cord segments L6, S1 receiving urethral afferent input, and L4 as a negative control, were dissected and processed for immunohistochemistry as described above. Tissue from two mice in which no surgical manipulations were performed was also collected. Previous studies suggested that 5-HT may diffuse through the epithelium, which has a lower resistance barrier compared to the bladder urothelium, and reach the sensory nerves.[73] However, we cannot exclude indirect effects due to 5-HT activation of epithelial cells which then release other transmitters that activate sensory nerves (Fig. 7).

Quantification of pERK$^+$ cells in the spinal cord L6 and L4 segments

Images were taken with 10× 0.4NA and 20× 0.7NA air objectives using a BX-62 Olympus upright fluorescent microscope. A threshold function was applied to reduce background staining using background levels from the sections incubated without the primary antibody. The total number of pERK$^+$ neurones in regions receiving input from urethral afferents (superficial dorsal horn, sacral parasympathetic nucleus and dorsal commissure)[12] was counted in every fourth section in two to five sections per segment per mouse by an experimenter blinded to the treatment. The average for each mouse was calculated and used for data analysis. Statistical comparisons were made using one-way ANOVA followed by Dunnett's multiple comparisons test among the three experimental groups (saline – V, AA and 5-HT). In a limited number of experiments, co-staining with the neuronal marker Tuj 1 (Neurone-specific class III beta-tubulin) was performed to determine that pERK$^+$ cells are neurones.

Visceromotor reflexes (VMRs)

VMR recordings were performed as previously described.[52] The VMR is a spinobulbospinal reflex, and its assessment consists of electromyographic (EMG) recordings of the abdominal musculature in response to distention of a visceral organ, in our case the urethra. Mice (n = 12) received urethane anaesthesia (1.5 mg kg^{-1}, i.p.). Two fine-insulated silver wire electrodes (0.05 mm diameter, A-M Systems, Everett, WA, USA) with exposed tips were embedded and secured into the left abdominal external oblique muscle. The sampling rate was set to 1 kHz for the EMG channel. A PE50 catheter was inserted into the urethra through the bladder dome and secured at the bladder neck as described above (schematic in Fig. 6d). The bladder was cut open to avoid any influences to the VMR. The catheter was connected via a three-way connector with a syringe pump and a pressure sensor, to infuse room temperature 0.9% NaCl and measure urethral pressure respectively. With urethra occluded, VMRs were measured during intra-urethral distention (IUD) from 0 to 40 cmH_2O in 10 cmH_2O increments for a duration of 120 s per step. In control mice, the urethra was distended with the saline vehicle (n = 4 mice). In the other animals, the urethra was first perfused with acetic acid (AA; 1%; n = 4 mice) or 5-HT (1 μM; n = 4 mice) for 30 min with urethra occluded, and then IUD conducted as described above, while maintaining AA or 5-HT within the urethra. Urethral pressure and VMRs were recorded by a data acquisition system (MP150; Biopac Systems, Goleta, CA, USA). For analysis, 10-s duration of the VMR area under the curve (AUC) during IUD was quantified for each level of urethral pressure. One-way ANOVA followed by the Dunn's multiple comparisons test was performed among the three experimental groups (saline, AA and 5-HT).

Dye labelling for identification of urethral primary afferent neurones

Urethral afferents were labelled by retrograde axonal transport of the fluorescent dye FAST DiI™ oil (DiIΔ9,12-C18(3), ClO4; 1,1′-Dilinoleyl-3,3,3′,3′-Tetramethylindocarbocyanine Perchlorate; Life Sciences cat # D3899, Thermo Fisher Scientific Corporation), a lipophilic fluorescent tracer, which is picked up by the nerves and retrogradely transported to the L6-S1 dorsal root ganglia (DRG), where the soma of primary afferent neurones are located.[74] Under isoflurane anaesthesia (2–3% in O_2), the bladder and urethra were exposed via a laparotomy. The dye was injected into multiple sites in the urethral wall (three to five sites, total volume 8–10 μL) using an insulin syringe. The injection sites were rinsed with saline to eliminate dye leakage and the incision sutured. All surgeries were performed in between 9 and 12 pm, and mice were allowed to recover on warm pads for 2–3 h prior to returning to the animal facility. The animals were treated with prophylactic antibiotic (Polyflex, 100 mg kg^{-1} s.c. 5–7 days; Boehringer Ingelheim Vetmedica, St. Joseph, MO, USA) and analgesic (carprofen, 5 mg kg^{-1} s.c.; 3–5 days; Zoetis, Kalamazoo, MI, USA) per veterinarian recommendation. Transport of the dye was allowed for 5–15 days.

Neuronal dissociation

Under isoflurane anaesthesia (5% in O_2), a laminectomy was performed and L6 and S1 DRGs were collected from eight mice injected with FAST DiI in the urethra. Ganglia were placed in Neurobasal A Medium (Thermo Fisher Scientific Corporation) with 5% B27 supplements and 0.5 mM L-glutamine, minced and enzymatically digested at 37 °C for 10–

20 min in Neurobasal A containing 1 mg mL^{-1} trypsin and 2 mg mL^{-1} collagenase type 4 (Worthington Biochemical, Lakewood, NJ, USA). The ganglia were then dissociated mechanically by trituration, washed with Neurobasal A and centrifuged three times for 5 min at 416G. The supernatant was removed and cells plated on polylysine-coated glass coverslips and kept in a 95% air and 5% CO_2 incubator at 37 °C until recording. Cells were used within 4–24 h after dissociation.

Calcium imaging

Imaging was performed as previously described.[75] DRG neurones were loaded with fura-2 AM (2 μM; Thermo Fisher Scientific Corporation) for 30 min at 37 °C in an atmosphere of 5% CO_2. Fura-2 AM was dissolved in the bath solution (Hanks Buffer Salt Solution, HBSS) containing in mM: NaCl 138, KCl 5, KH_2PO_4 0.3, $NaHCO_3$ 4, $CaCl_2$ 2, $MgCl_2$ 1, HEPES 10, glucose 5.6, pH 7.4, 310 mOsm L^{-1}) to which bovine serum albumin (BSA, 5 mg mL^{-1}; Sigma-Aldrich) was added to promote dye loading. Coverslips were placed on an inverted epifluorescence microscope (Olympus IX70) and continuously super-fused with HBSS. Fura-2 was excited alternately at 340/380 nm, and fluorescence emission was detected at 510 nm using a computer-controlled monochromator running under HCIMAGE software. Drugs were dissolved in external solution and delivered via bath application using a gravity-driven application system positioned within close proximity to imaged cells. To examine repeatability of 5-HT responses, 5-HT (1 μM) was applied every 15 min. For the experiments using antagonists (ritanserin and Y-25130; 1 μM), a response to 5-HT was first obtained, then cells were perfused for 15 min with each antagonist and tested again with 5-HT. The control vehicle (0.01% DMSO used for dissolving capsaicin) did not alter the intracellular calcium concentration ($[Ca^{2+}]_i$). Digital images were analysed using HCIMAGEsoftware. Only cells responding to KCl (50 mM) were included in analysis. The amplitude of the response, expressed as changes in R (F_{340}/F_{380}) before and after drug application, was analysed. Results are given as percentage increase in R above resting $[Ca^{2+}]_i$ levels (ΔR/R). Statistical comparisons were made using paired *t*-test, unpaired *t*-test or Fisher's exact test, as noted in the text and figure legends.

Statistical analysis

Results are expressed as mean ± SEM. Values for control vs. drug treatment were evaluated with statistical tests indicated in the text and figure legends, using GRAPHPAD PRISM 6 (GraphPad Software, La Jolla, CA, USA). $P < 0.05$ was considered statistically significant. * indicates $P < 0.05$; † indicates $P < 0.01$ and ‡ indicates $P < 0.001$.

Acknowledgments

The authors thank Wily G. Ruiz for technical assistance with confocal imaging, Amanda Wolf-Johnston for ordering supplies and Dr. Larissa Rodriguez for providing support for Drs. Huiyi Chang and Jih-Chao Yeh. We also thank Dr. Marcelo Carattino for critical reading of the manuscript. This research was supported by the following grants: Samuel & Emma Winters Foundation to FAK, P30 DK079307 Pittsburgh Center for Kidney Research – O'Brien Pilot to FAK, P30 DK079307 Pittsburgh Center for Kidney Research – the Kidney Imaging Core to GA, RO1 DK54425 to GA, R01 DK106181 to HHC, RO1 DK57284 and R37 DK54824 to LAB.

References

1. Maksimovic S, Nakatani M, Baba Y, Nelson AM, Marshall KL, Wellnitz SA, Firozi P, Woo SH, Ranade S, Patapoutian A, Lumpkin EA. Epidermal Merkel cells are mechanosensory cells that tune mammalian touch receptors. Nature. 2014; 509:617–621. [PubMed: 24717432]
2. Danziger ZC, Grill WM. Sensory and circuit mechanisms mediating lower urinary tract reflexes. Auton Neurosci. 2016; 200:21–28. [PubMed: 26119358]
3. de Groat WC, Fraser MO, Yoshiyama M, Smerin S, Tai C, Chancellor MB, Yoshimura N, Roppolo JR. Neural control of the urethra. Scand J Urol Nephrol Suppl. 2001; 207:35–43. discussion 106–125.
4. Eggermont M, Wyndaele JJ, Gillespie J, De Wachter S. Response properties of urethral distension evoked unifiber afferent potentials in the lower urinary tract. J Urol. 2015; 194:1473–1480. [PubMed: 26055821]
5. Snellings AE, Yoo PB, Grill WM. Urethral flow-responsive afferents in the cat sacral dorsal root ganglia. Neurosci Lett. 2012; 516:34–38. [PubMed: 22480694]
6. Bahns E, Ernsberger U, Janig W, Nelke A. Functional characteristics of lumbar visceral afferent fibres from the urinary bladder and the urethra in the cat. Pflugers Arch. 1986; 407:510–518. [PubMed: 3786110]
7. Shafik A, el-Sibai O, Ahmed I. Effect of urethral dilation on vesical motor activity: identification of the urethrovesical reflex and its role in voiding. J Urol. 2003; 169:1017–1019. [PubMed: 12576835]
8. Shafik A, Shafik AA, El-Sibai O, Ahmed I. Role of positive urethrovesical feedback in vesical evacuation. The concept of a second micturition reflex: the urethrovesical reflex. World J Urol. 2003; 21:167–170. [PubMed: 12898170]
9. Wyndaele JJ. The normal pattern of perception of bladder filling during cystometry studied in 38 young healthy volunteers. J Urol. 1998; 160:479–481. [PubMed: 9679902]
10. Wyndaele J-J, Van de Borne S, Wyndaele M, De Wachter S. Sensation in the urethra during voiding studied in young healthy men. Bladder. 2016; 3:1–4.
11. Birder LA, de Wachter S, Gillespie J, Wyndaele JJ. Urethral sensation: basic mechanisms and clinical expressions. Int J Urol. 2014; 21(Suppl 1):13–16. [PubMed: 24807486]
12. Birder LA, de Groat WC. Increased c-fos expression in spinal neurons after irritation of the lower urinary tract in the rat. J Neurosci. 1992; 12:4878–4889. [PubMed: 1464772]
13. Conte B, Maggi CA, Giachetti A, Parlani M, Lopez G, Manzini S. Intraurethral capsaicin produces reflex activation of the striated urethral sphincter in urethane-anesthetized male rats. J Urol. 1993; 150:1271–1277. [PubMed: 8371414]
14. Deckmann K, Filipski K, Krasteva-Christ G, Fronius M, Althaus M, Rafiq A, Papadakis T, Renno L, Jurastow I, Wessels L, Wolff M, Schutz B, Weihe E, Chubanov V, Gudermann T, Klein J, Bschleipfer T, Kummer W. Bitter triggers acetylcholine release from polymodal urethral chemosensory cells and bladder reflexes. Proc Natl Acad Sci USA. 2014; 111:8287–8292. [PubMed: 24843119]
15. Thor KB, Muhlhauser MA. Vesicoanal, urethroanal, and urethrovesical reflexes initiated by lower urinary tract irritation in the rat. Am J Physiol. 1999; 277:R1002–R1012. [PubMed: 10516238]
16. Robain G, Combrisson H, Mazieres L. Bladder response to urethral flow in the awake ewe. Neurourol Urodyn. 2001; 20:641–649. [PubMed: 11574939]
17. Conte B, Maggi CA, Meli A. Vesico-inhibitory responses and capsaicin-sensitive afferents in rats. Naunyn Schmiedebergs Arch Pharmacol. 1989; 339:178–183. [PubMed: 2725696]
18. Conte B, Maggi CA, Parlani M, Giachetti A. Evidence for the existence of a urethro-urethral excitatory reflex in urethane anesthetized rats: involvement of peripheral ganglionic structures. J Urol. 1991; 146:1627–1630. [PubMed: 1682514]
19. Kennelly MJ, Arena KC, Shaffer N, Bennett ME, Grill WM, Grill JH, Boggs JW. Electrical stimulation of the urethra evokes bladder contractions in a woman with spinal cord injury. J Spinal Cord Med. 2010; 33:261–265. [PubMed: 20737800]
20. Danziger ZC, Grill WM. Dynamics of the sensory response to urethral flow over multiple time scales in rat. J Physiol. 2015; 593:3351–3371. [PubMed: 26041695]

21. Kamo I, Cannon TW, Conway DA, Torimoto K, Chancellor MB, de Groat WC, Yoshimura N. The role of bladder-to-urethral reflexes in urinary continence mechanisms in rats. Am J Physiol Renal Physiol. 2004; 287:F434–F441. [PubMed: 15113743]
22. Abelli L, Conte B, Somma V, Parlani M, Geppetti P, Maggi CA. Mechanical irritation induces neurogenic inflammation in the rat urethra. J Urol. 1991; 146:1624–1626. [PubMed: 1719251]
23. Liedberg H. Catheter induced urethral inflammatory reaction and urinary tract infection. An experimental and clinical study. Scand J Urol Nephrol Suppl. 1989; 124:1–43. [PubMed: 2633310]
24. Nordling L, Liedberg H, Ekman P, Lundeberg T. Influence of the nervous system on experimentally induced urethral inflammation. Neurosci Lett. 1990; 115:183–188. [PubMed: 2234496]
25. Nordling L, Lundeberg T, Brolin J, Liedberg H, Ekman P, Theodorsson E. The role of sensory nerves in catheter-induced urethral inflammation. Eur Urol. 1992; 21:75–78.
26. Di Sant'Agnese PA, Davis NS, Chen M, de Mesy Jensen KL. Age-related changes in the neuroendocrine (endocrine-paracrine) cell population and the serotonin content of the guinea pig prostate. Lab Invest. 1987; 57:729–736. [PubMed: 3695416]
27. di Sant'Agnese PA, de Mesy Jensen KL. Endocrine-paracrine (APUD) cells of the human female urethra and paraurethral ducts. J Urol. 1987; 137:1250–1254. [PubMed: 2438433]
28. Hakanson R, Larsson LI, Sjoberg NO, Sundler F. Amine-producing endocrine-like cells in the epithelium of urethra and prostate of the guinea-pig. A chemical, fluorescence histochemical, and electron microscopic study. Histochemie. 1974; 38:259–270. [PubMed: 4134747]
29. Hanyu S, Iwanaga T, Kano K, Fujita T. Distribution of serotonin-immunoreactive paraneurons in the lower urinary tract of dogs. Am J Anat. 1987; 180:349–356. [PubMed: 3425562]
30. Iwanaga T, Han H, Hoshi O, Kanazawa H, Adachi I, Fujita T. Topographical relation between serotonin-containing paraneurons and peptidergic neurons in the intestine and urethra. Biol Signals. 1994; 3:259–270. [PubMed: 7704106]
31. Iwanaga T, Hanyu S, Fujita T. Serotonin-immunoreactive cells of peculiar shape in the urethral epithelium of the human penis. Cell Tissue Res. 1987; 249:51–56. [PubMed: 2441867]
32. Vittoria A, La Mura E, Cocca T, Cecio A. Serotonin-, somatostatin- and chromogranin A-containing cells of the urethro-prostatic complex in the sheep. An immunocytochemical and immunofluorescent study. J Anat. 1990; 171:169–178. [PubMed: 1981998]
33. Yokoyama T, Saino T, Nakamuta N, Yamamoto Y. Topographic distribution of serotonin-immunoreactive urethral endocrine cells and their relationship with calcitonin gene-related peptide-immunoreactive nerves in male rats. Acta Histochem. 2017; 119:78–83. [PubMed: 27939448]
34. Fujita, T. The gastro-enteric endocrine cells and its paraneuronic nature. In: Coupland, RE., Fujita, T., editors. Chromaffin, Enterochromaffin and Related Cells. Amsterdam: Elesevier; 1976. p. 191-208.
35. Kummer W, Deckmann K. Brush cells, the newly identified gatekeepers of the urinary tract. Curr Opin Urol. 2017; 27:85–92. [PubMed: 27846033]
36. Deckmann K, Kummer W. Chemosensory epithelial cells in the urethra: sentinels of the urinary tract. Histochem Cell Biol. 2016; 146:673–683. [PubMed: 27680547]
37. Evergren E, Benfenati F, Shupliakov O. The synapsin cycle: a view from the synaptic endocytic zone. J Neurosci Res. 2007; 85:2648–2656. [PubMed: 17455288]
38. Browning KN. Role of central vagal 5-HT3 receptors in gastrointestinal physiology and pathophysiology. Front Neurosci. 2015; 9:413. [PubMed: 26578870]
39. Christian EP, Taylor GE, Weinreich D. Serotonin increases excitability of rabbit C-fiber neurons by two distinct mechanisms. J Appl Physiol (1985). 1989; 67:584–591. [PubMed: 2793660]
40. Holz GG, Shefner SA, Anderson EG. Serotonin depolarizes type A and C primary afferents: an intracellular study in bullfrog dorsal root ganglion. Brain Res. 1985; 327:71–79. [PubMed: 3872695]
41. Nicholson R, Small J, Dixon AK, Spanswick D, Lee K. Serotonin receptor mRNA expression in rat dorsal root ganglion neurons. Neurosci Lett. 2003; 337:119–122. [PubMed: 12536038]

42. Sasaki M, Ishizaki K, Obata H, Goto F. Effects of 5-HT2 and 5-HT3 receptors on the modulation of nociceptive transmission in rat spinal cord according to the formalin test. Eur J Pharmacol. 2001; 424:45–52. [PubMed: 11470259]
43. Zeitz KP, Guy N, Malmberg AB, Dirajlal S, Martin WJ, Sun L, Bonhaus DW, Stucky CL, Julius D, Basbaum AI. The 5-HT3 subtype of serotonin receptor contributes to nociceptive processing via a novel subset of myelinated and unmyelinated nociceptors. J Neurosci. 2002; 22:1010–1019. [PubMed: 11826129]
44. Glennon RA. Serotonin receptors and site-selective agents. J Physiol Pharmacol. 1991; 42:49–60. [PubMed: 1932772]
45. Cruz CD, Cruz F. The ERK 1 and 2 pathway in the nervous system: from basic aspects to possible clinical applications in pain and visceral dysfunction. Curr Neuropharmacol. 2007; 5:244–252. [PubMed: 19305741]
46. DeBerry JJ, Saloman JL, Dragoo BK, Albers KM, Davis BM. Artemin immunotherapy is effective in preventing and reversing cystitis-induced bladder hyperalgesia via TRPA1 regulation. J Pain. 2015; 16:628–636. [PubMed: 25892657]
47. Ji RR, Gereau RWt, Malcangio M, Strichartz GR. MAP kinase and pain. Brain Res Rev. 2009; 60:135–148. [PubMed: 19150373]
48. Lai HH, Qiu CS, Crock LW, Morales ME, Ness TJ, Gereau RWt. Activation of spinal extracellular signal-regulated kinases (ERK) 1/2 is associated with the development of visceral hyperalgesia of the bladder. Pain. 2011; 152:2117–2124. [PubMed: 21705143]
49. Yoo CJ, Hwang SJ. The VR1-positive primary afferent-mediated expression of pERK in the lumbosacral neurons in response to mechanical and chemical stimulation of the urinary bladder in rats. J Korean Neurosurg Soc. 2007; 42:462–469. [PubMed: 19096590]
50. Birder LA, de Groat WC. Induction of c-fos expression in spinal neurons by nociceptive and nonnociceptive stimulation of LUT. Am J Physiol. 1993; 265:R326–R333. [PubMed: 8368386]
51. Birder LA, de Groat WC. Contribution of C-fiber afferent nerves and autonomic pathways in the urinary bladder to spinal c-fos expression induced by bladder irritation. Somatosens Mot Res. 1998; 15:5–12. [PubMed: 9583573]
52. Chang HH, Havton LA. Modulation of the visceromotor reflex by a lumbosacral ventral root avulsion injury and repair in rats. Am J Physiol Renal Physiol. 2012; 303:F641–F647. [PubMed: 22696606]
53. Ness TJ, Elhefni H. Reliable visceromotor responses are evoked by noxious bladder distention in mice. J Urol. 2004; 171:1704–1708. [PubMed: 15017270]
54. Ness TJ, Lewis-Sides A, Castroman P. Characterization of pressor and visceromotor reflex responses to bladder distention in rats: sources of variability and effect of analgesics. J Urol. 2001; 165:968–974. [PubMed: 11176524]
55. Sadler KE, Stratton JM, Kolber BJ. Urinary bladder distention evoked visceromotor responses as a model for bladder pain in mice. J Vis Exp. 2014; 51413 https://doi.org/10.3791/51413.
56. Smith PP, Kuchel GA. Continuous uroflow cystometry in the urethane-anesthetized mouse. Neurourol Urodyn. 2010; 29:1344–1349. [PubMed: 20127833]
57. Garcia-Pascual A, Sancho M, Costa G, Triguero D. Interstitial cells of Cajal in the urethra are cGMP-mediated targets of nitrergic neurotransmission. Am J Physiol Renal Physiol. 2008; 295:F971–F983. [PubMed: 18632793]
58. Sancho M, Garcia-Pascual A, Triguero D. Presence of the Ca2 + -activated chloride channel anoctamin 1 in the urethra and its role in excitatory neurotransmission. Am J Physiol Renal Physiol. 2012; 302:F390–F400. [PubMed: 22114201]
59. Dixon JS, Gosling JA, Ramsdale DR. Urethral chromaffin cells. A light and electron microscopic study. Z Zellforsch Mikrosk Anat. 1973; 138:397–406. [PubMed: 4735903]
60. Ramsdale DR. Further observations on urethral chromaffin cells: an electron microscopic study. Cell Tissue Res. 1974; 148:499–504. [PubMed: 4365460]
61. Press D, Mutlu S, Guclu B. Evidence of fast serotonin transmission in frog slowly adapting type 1 responses. Somatosens Mot Res. 2010; 27:174–185. [PubMed: 20937000]

62. He L, Tuckett RP, English KB. 5-HT2 and 3 receptor antagonists suppress the response of rat type I slowly adapting mechanoreceptor: an *in vitro* study. Brain Res. 2003; 969:230–236. [PubMed: 12676383]
63. Maksimovic S, Baba Y, Lumpkin EA. Neurotransmitters and synaptic components in the Merkel cell-neurite complex, a gentle-touch receptor. Ann N Y Acad Sci. 2013; 1279:13–21. [PubMed: 23530998]
64. Bardin L. The complex role of serotonin and 5-HT receptors in chronic pain. Behav Pharmacol. 2011; 22:390–404. [PubMed: 21808193]
65. Manocha M, Khan WI. Serotonin and GI disorders: an update on clinical and experimental studies. Clin Transl Gastroenterol. 2012; 3:e13. [PubMed: 23238212]
66. Mawe GM, Hoffman JM. Serotonin signalling in the gut-functions, dysfunctions and therapeutic targets. Nat Rev Gastroenterol Hepatol. 2013; 10:473–486. [PubMed: 23797870]
67. Bertrand PP, Bertrand RL. Serotonin release and uptake in the gastrointestinal tract. Auton Neurosci. 2010; 153:47–57. [PubMed: 19729349]
68. Bachmann LH, Manhart LE, Martin DH, Sena AC, Dimitrakoff J, Jensen JS, Gaydos CA. Advances in the understanding and treatment of male urethritis. Clin Infect Dis. 2015; 61(Suppl 8):S763–S769. [PubMed: 26602615]
69. Henderson L, Farrelly P, Dickson AP, Goyal A. Management strategies for idiopathic urethritis. J Pediatr Urol. 2016; 12:35, e31–35. [PubMed: 26257028]
70. Tritschler S, Roosen A, Fullhase C, Stief CG, Rubben H. Urethral stricture: etiology, investigation and treatments. Dtsch Arztebl Int. 2013; 110:220–226. [PubMed: 23596502]
71. Julius D, Basbaum AI. Molecular mechanisms of nociception. Nature. 2001; 413:203–210. [PubMed: 11557989]
72. Persson PB. Good publication practice in physiology 2015. Acta Physiol (Oxf). 2015; 215:163–164. [PubMed: 26384745]
73. Ishigami T, Yoshioka K, Karicheti V, Marson L. A role for peripheral 5-HT2 receptors in serotonin-induced facilitation of the expulsion phase of ejaculation in male rats. J Sex Med. 2013; 10:2688–2702. [PubMed: 24024794]
74. Yoshimura N, Seki S, Erickson KA, Erickson VL, Hancellor MB, de Groat WC. Histological and electrical properties of rat dorsal root ganglion neurons innervating the lower urinary tract. J Neurosci. 2003; 23:4355–4361. [PubMed: 12764124]
75. Kullmann FA, Artim D, Beckel J, Barrick S, de Groat WC, Birder LA. Heterogeneity of muscarinic receptor-mediated Ca2 + responses in cultured urothelial cells from rat. Am J Physiol Renal Physiol. 2008; 294:F971–F981. [PubMed: 18272602]
76. Ptak K, Yamanishi T, Aungst J, Milescu LS, Zhang R, Richerson GB, Smith JC. Raphe neurons stimulate respiratory circuit activity by multiple mechanisms via endogenously released serotonin and substance P. J Neurosci. 2009; 29:3720–3737. [PubMed: 19321769]
77. Gomez C, David V, Peet NM, Vico L, Chenu C, Malaval L, Skerry TM. Absence of mechanical loading in utero influences bone mass and architecture but not innervation in Myod-Myf5-deficient mice. J Anat. 2007; 210:259–271. [PubMed: 17331176]
78. Brouns I, Oztay F, Pintelon I, De Proost I, Lembrechts R, Timmermans JP, Adriaensen D. Neurochemical pattern of the complex innervation of neuroepithelial bodies in mouse lungs. Histochem Cell Biol. 2009; 131:55–74. [PubMed: 18762965]
79. Schnizler K, Shutov LP, Van Kanegan MJ, Merrill MA, Nichols B, McKnight GS, Strack S, Hell JW, Usachev YM. Protein kinase A anchoring via AKAP150 is essential for TRPV1 modulation by forskolin and prostaglandin E2 in mouse sensory neurons. J Neurosci. 2008; 28:4904–4917. [PubMed: 18463244]
80. Mellott JG, Bickford ME, Schofield BR. Descending projections from auditory cortex to excitatory and inhibitory cells in the nucleus of the brachium of the inferior colliculus. Front Syst Neurosci. 2014; 8:188. [PubMed: 25339870]
81. Al-Noah Z, McKenna D, Langdale C, Thor KB, Marson L, Burgard E, Kullmann FA. Nitrergic relaxations and phenylephrine contractions are not compromised in isolated urethra in a rat model of diabetes. Auton Neurosci. 2014; 183:58–65. [PubMed: 24656892]

82. Langdale CL, Thor KB, Marson L, Burgard EC. Maintenance of bladder innervation in diabetes: a stereological study of streptozotocin-treated female rats. Auton Neurosci. 2014; 185:59–66. [PubMed: 25066250]

83. Schiwy N, Brazda N, Muller HW. Enhanced regenerative axon growth of multiple fibre populations in traumatic spinal cord injury following scar-suppressing treatment. Eur J Neurosci. 2009; 30:1544–1553. [PubMed: 19817844]

84. Guo F, Ma J, McCauley E, Bannerman P, Pleasure D. Early postnatal proteolipid promoter-expressing progenitors produce multilineage cells *in vivo*. J Neurosci. 2009; 29:7256–7270. [PubMed: 19494148]

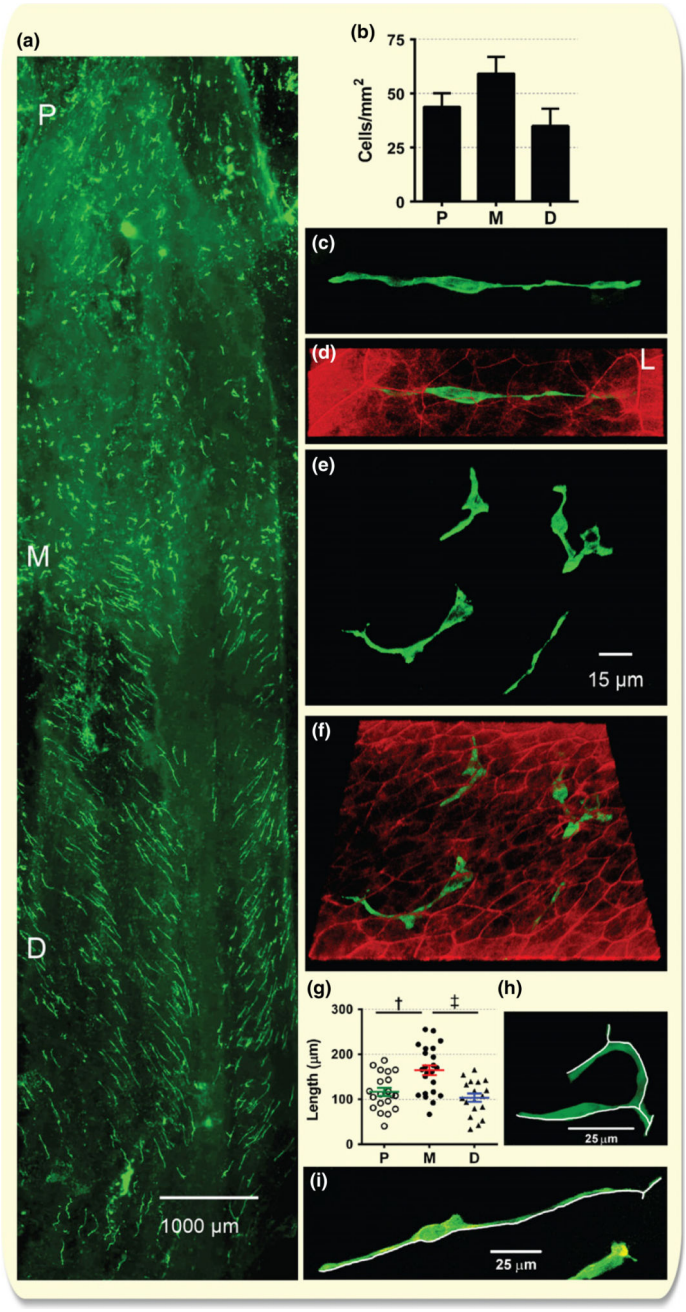

Figure 1.

Distribution and morphology of 5-HT$^+$ paraneurones. (a) Wholemount urethra stained for 5-HT. The epithelium is facing upright. P, M and D indicate proximal, mid and distal areas of the urethra. To cover the entire urethra, multiple images as single optical sections were acquired with a 5× 0.15NA air objective and assembled using the mosaic function in IMAGEJ. (b) Density of 5-HT $^+$ cells along the urethral length (one-way ANOVA, $F(2,9) = 2.732$, $P = 0.118$). Cells were counted from four whole-mount urethrae. (c) Example of a 5-HT$^+$ cell in the mid-urethra, illustrating bipolar-like processes. (d) Co-staining with phalloidin (red) to delineate the epithelium illustrates 5-HT$^+$ processes (green) embedded in the epithelium and

oriented parallel to the lumen (L). (e). Example of a 5-HT$^+$ cell in the proximal urethra, illustrating multipolar-like cells. (f) Co-staining with phalloidin (red) to delineate the epithelium illustrates 5-HT$^+$ processes (green) spanning the epithelium in different directions. Scale bar for (c–f) is illustrated in panel (e). Images in panels (c–f) are 3D reconstructions of confocal images taken with a 63× 1.3NA glycerol objective using Z steps of 0.5 μm. L stands for the lumen of the urethra. (g) Total length of cell including processes for cells located in the proximal, mid- and distal urethra. † and ‡ indicate statistically significant differences tested with one-way ANOVA: $F(2,58) = 10.67$, $P = 0.0001$, followed by Tukey's multiple comparisons test: P vs. M $P = 0.0028$ and D vs. M, $P = 0.0002$). (h, i) Examples of cell tracing – white line – from distal urethra (h) and mid-urethra (i) used for calculation of the total length.

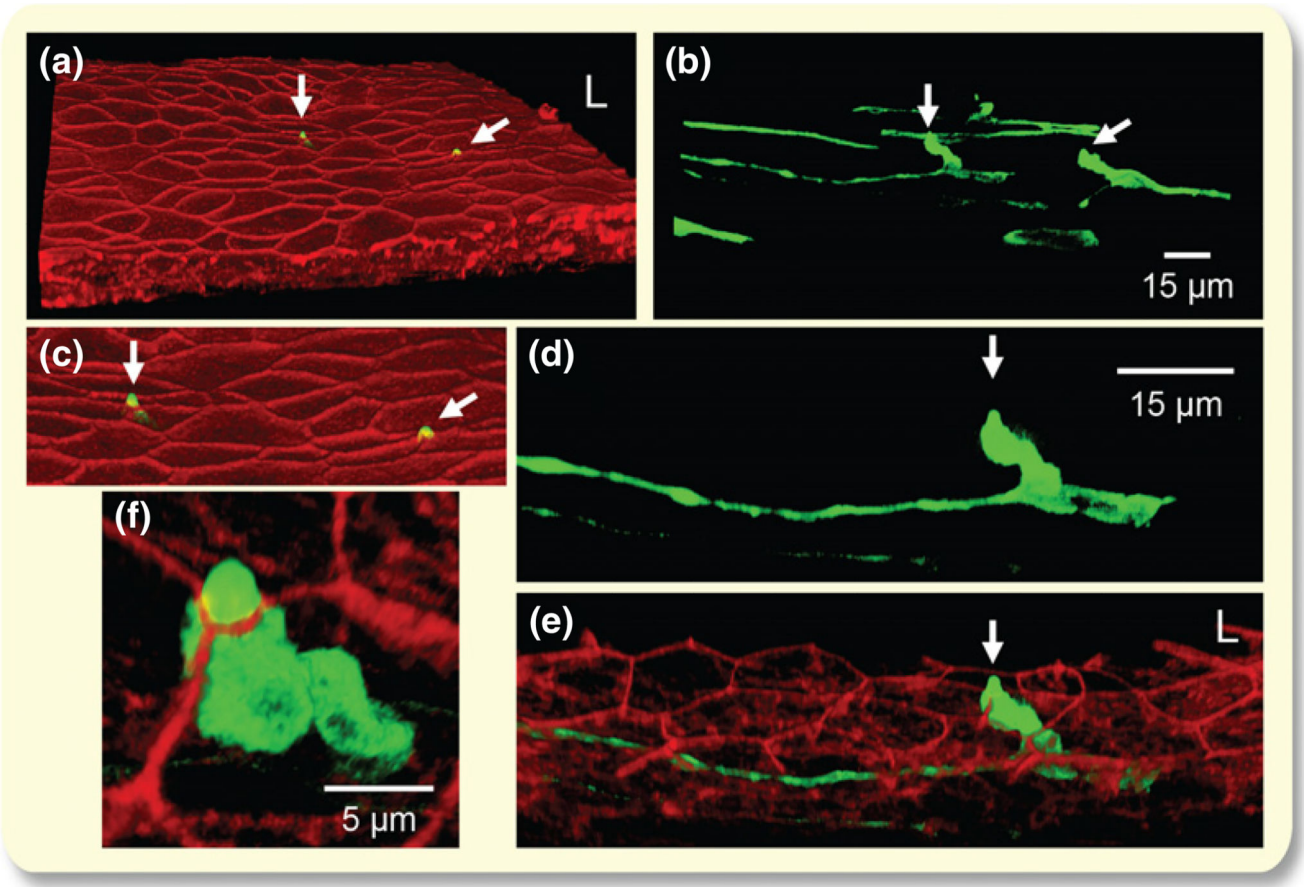

Figure 2.

Processes of 5-HT$^+$ cells reaching the lumen. (a) View of the luminal surface of the epithelium stained with phalloidin (red) illustrating processes of two 5-HT$^+$ cells (green; arrows) penetrating through the epithelium to reach the lumen (L). Example is from the mid-urethral area. (b) 3D confocal reconstruction (Z-stacks of 0.5 μm steps) of 5-HT$^+$ cells (green) embedded in the epithelium in the example from panel (a). Arrows point to the processes penetrating the lumen. Scale for panels (a), (b) is the same and is illustrated in (b). (c) High magnification view of the epithelium and penetrating processes. (d–f) High magnification view of the cell marked by perpendicular arrow. Note the penetration of the epithelium to reach the lumen at the intersection of large epithelial cells.

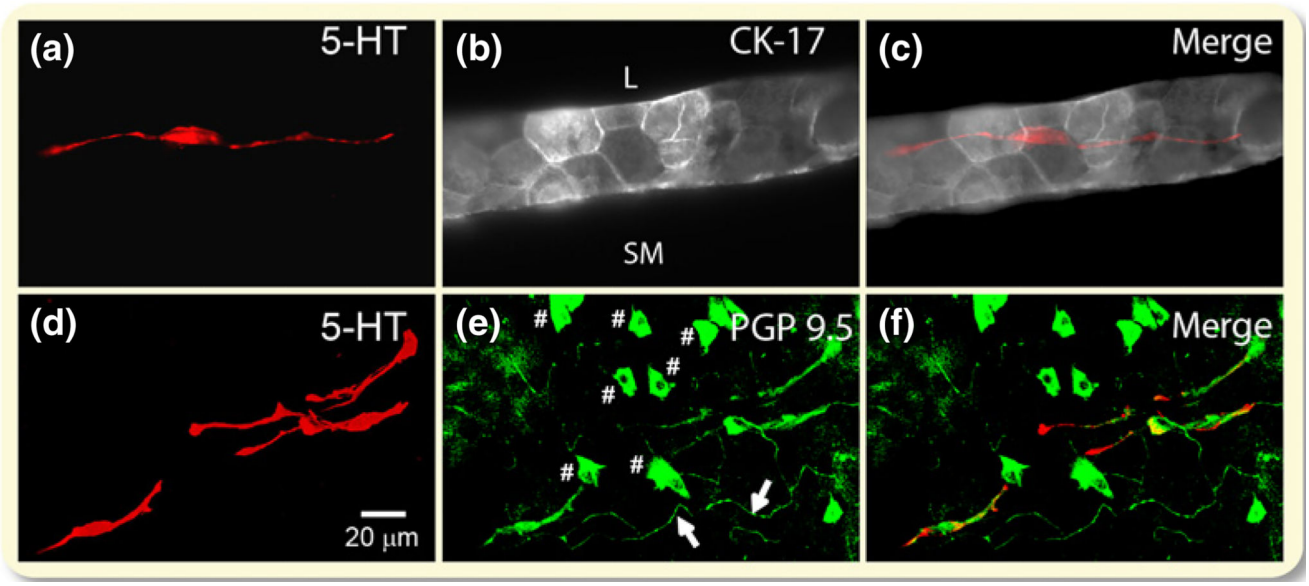

Figure 3.

Neurone-like characteristics of 5-HT$^+$ cells. (a–c) 5-HT$^+$ paraneurones (red) do not exhibit immunoreactivity for cytokeratin 17, a marker of epithelial cells. Note the epithelium composed of ~2–3 layers of cytokeratin 17-positive cells (grey staining). L stands for lumen and SM for smooth muscle. Staining was performed in transverse sections. Images are single optical sections acquired with a 20× 0.7NA air objective. (d–f) 5-HT$^+$ paraneurones exhibit immunoreactivity for PGP9.5, a neuronal marker. Nerve fibres are visible in green; # indicates other cells that stain positive for PGP9.5, presumed non-serotonergic paraneurones. Staining was performed in whole-mount urethra. The urethral lumen is facing up. Images are maximum projection of Z-stacks of 0.25-μm steps acquired with a 63× 1.3NA glycerol objective. The scale bar is the same for all panels and it is illustrated in panel (d).

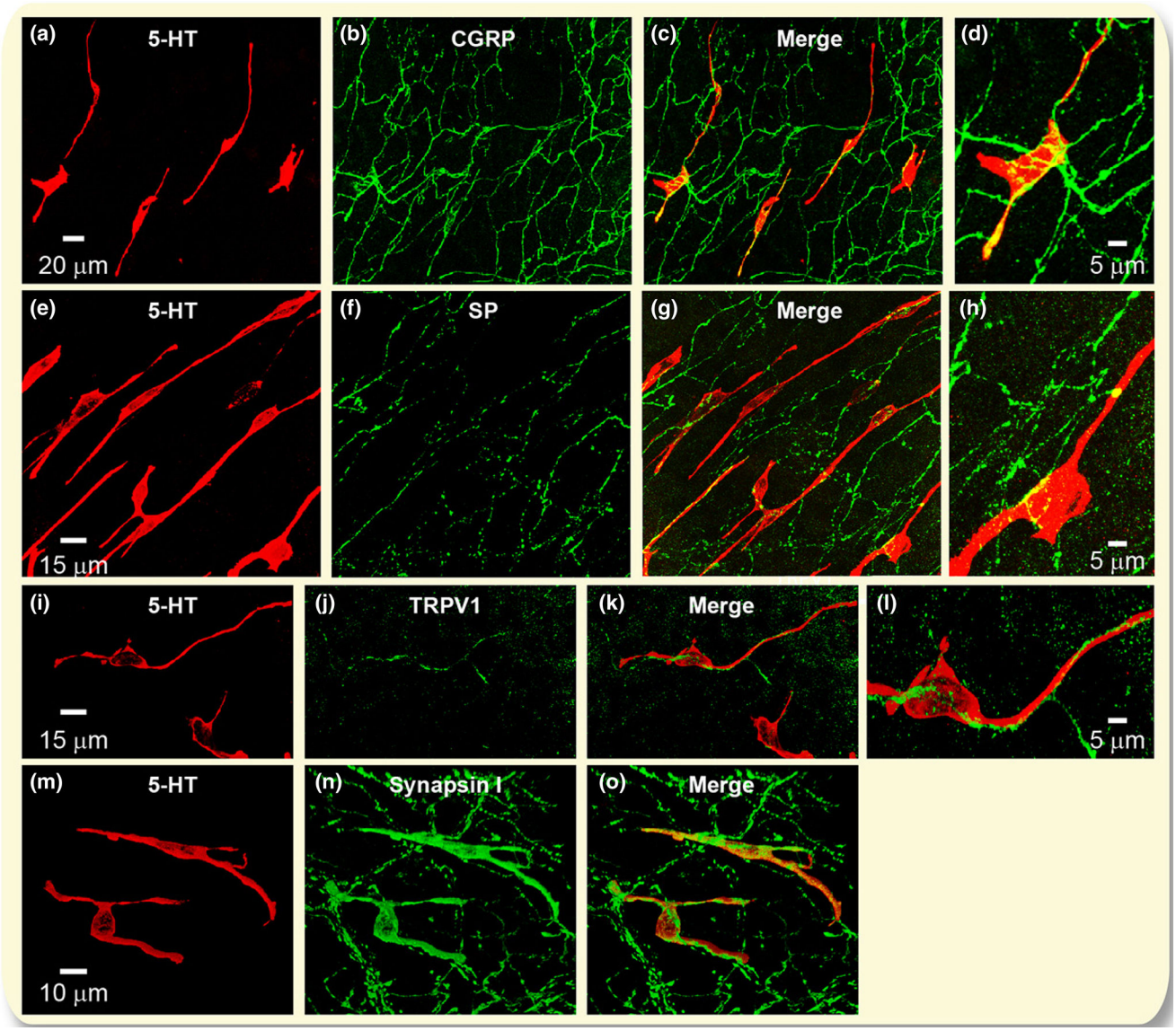

Figure 4.

Relationship between 5-HT$^+$ paraneurones and afferent nerve fibres. (a–d) Relationship with CGRP$^+$ fibres. (a) 5-HT$^+$ cells (red). (b) CGRP$^+$ nerve fibres (green). (c) Merge. Scale for panels a–c is illustrated in (a). (d) Enlargement from c, illustrating the close proximity and overlap (yellow) between 5-HT$^+$ cells and CGRP$^+$ fibres. (e–h) Relationship with SP$^+$ fibres. (e) 5-HT$^+$ cells (red). (f) SP$^+$ nerve fibres (green). (g) Merge. Scale for panels e–h is illustrated in (e). (h) Enlargement from g, illustrating close proximity between 5-HT$^+$ cells and SP$^+$ fibres. (i–l) Relationship with TRPV1$^+$ fibres. (i) 5-HT$^+$ cells (red). (j) TRPV1$^+$ nerve fibres (green). (k) Merge. Scale for panels i–l is illustrated in (i). (l) Enlargement from k, illustrating close proximity between 5-HT$^+$ cells and TRPV1$^+$ fibres. (m–n) Relationship with synapsin I$^+$ fibres. (m). 5-HT$^+$ cells (red). (n) Synapsin I$^+$ nerve fibres and paraneurones (green). Urethrae from three to six mice were used for each type of nerve fibre staining. All images are maximum projection of Z-stacks acquired with a 0.25-μm step using a 63× 1.3NA glycerol objective.

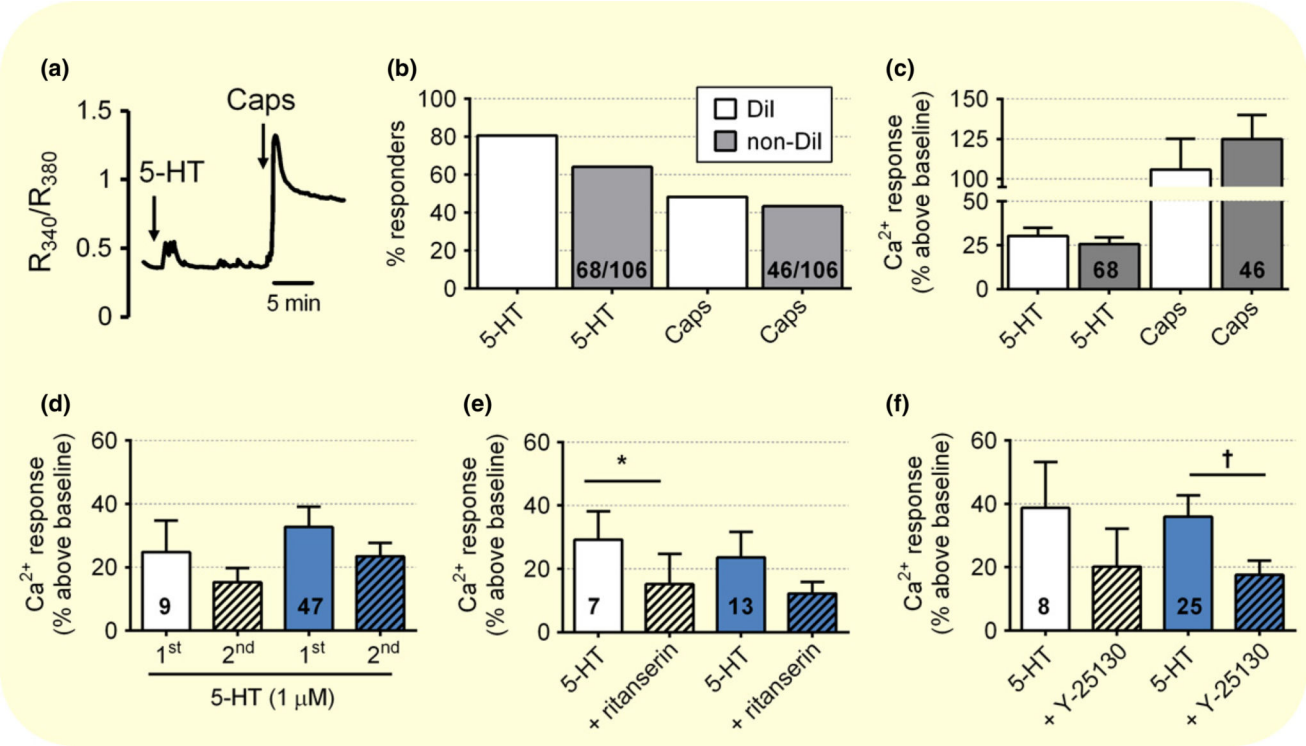

Figure 5.

Urethral primary afferent neurones respond to 5-HT. (a) Examples of changes in the $[Ca^{2+}]_i$ in response to 5-HT (1 μM) and capsaicin (caps; 0.5 μM) from a DiI-positive neurone. Drugs were applied at the time indicated by the arrow for 30 s. A total of eight mice injected with DiI in the urethra were used in these experiments. (b) Percentage of cells responding to 5-HT and capsaicin. Black bars represent DiI-positive neurones and grey bars, non-DiI-positive neurones. Numbers within the bars represent cell counts. No significant differences were noted between DiI and non-DiI cells in regard to responsiveness to 5-HT (Fisher's exact test $P = 0.49$). (c) Magnitude of calcium responses elicited by 5-HT and capsaicin in the DiI and non-DiI neurones. No statistically significant difference between the magnitude of the response in the DiI and non-DiI populations were noted (unpaired *t*-test $P = 0.49$). (d) Repeatability of 5-HT-induced responses. 5-HT was applied every 15 min. The second response was slightly but not significantly different from the first response in both populations (DiI: paired *t*-test $P = 0.39$, $n = 9$ cells; non-DiI: paired *t*-test $P = 0.0539$, $n = 47$ cells). (e) The non-selective 5-HT_2 antagonist, ritanserin (1 μM), decreases the responses to 5-HT (1 μM) in both population. Asterisk indicates statistically significant differences before and after antagonist (DiI: paired *t*-test $P = 0.025$, $n = 7$ cells; non-DiI: paired *t*-test $P = 0.1073$, $n = 13$ cells). (f) The specific 5-HT_3 receptor antagonist, Y-25130 hydrochloride (1 μM), decreases the responses to 5-HT (1 μM). † indicates statistically significant differences before and after antagonist (DiI: paired *t*-test $P = 0.1862$, $n = 8$ cells; non-DiI: paired *t*-test $P = 0.0097$, $n = 25$ cells).

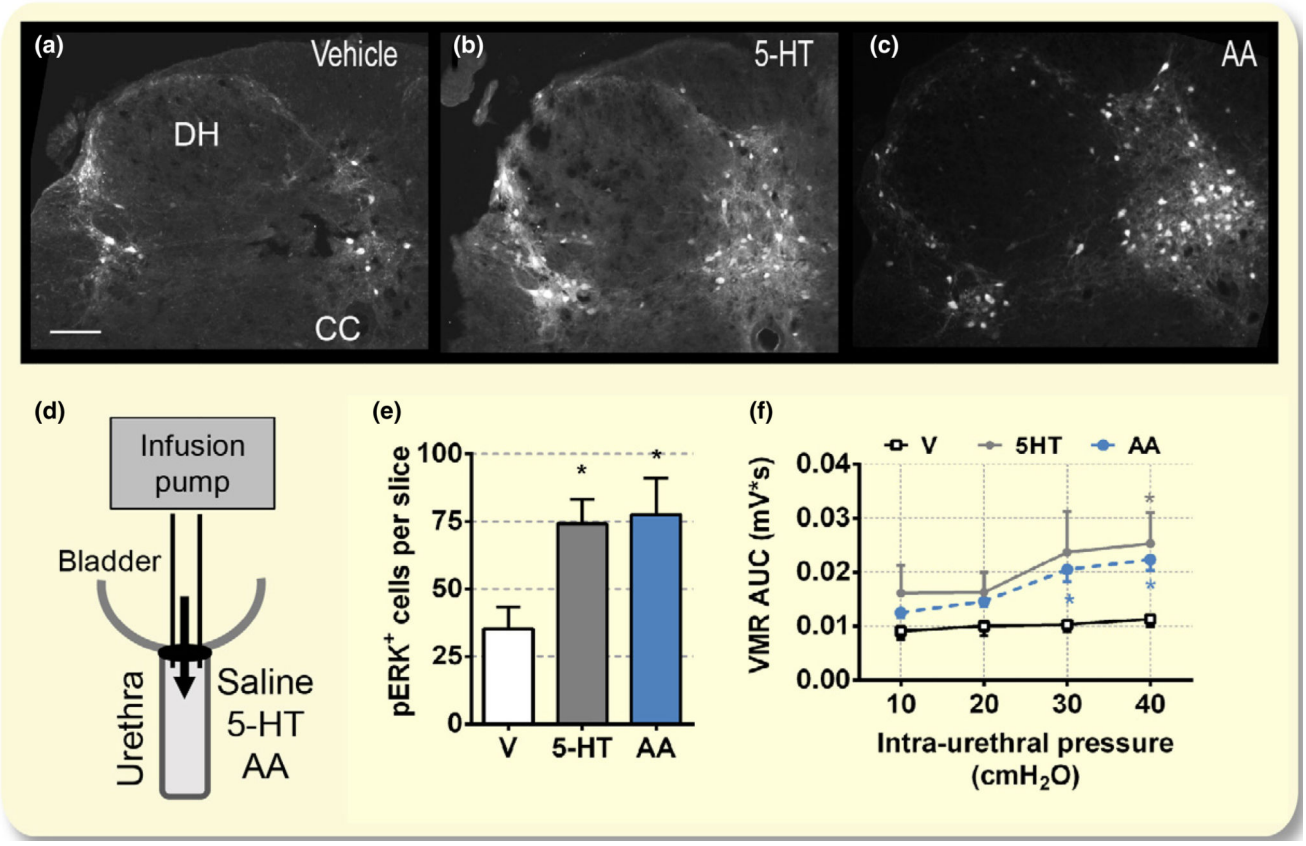

Figure 6.

Intra-urethral stimulation with 5-HT activates spinal nociceptive pathways. (a–c) Intra-urethral infusion of 5-HT (1 μM) increases pERK in the L6 spinal cord neurones. Example of dorsal horn spinal L6 cord sections from mice infused intra-urethrally with vehicle – saline (a), 5-HT (1 μM; b) and AA (1%; c). DH, dorsal horn and CC, central canal. Images presented are single optical sections taken with a 10× 0.4NA air objective. Scale is 100 μm. (d) Schematic of urethral perfusion. The bladder was cut open, and a PE50 catheter was advanced into the urethra and tied at the bladder neck. Perfusate (saline – V, 5-HT or AA) was infused into the urethra using a syringe pump. (e) Average number of $pERK^+$ cells per section, counted from two to five sections per mouse from six mice for vehicle group, nine mice for 5-HT group and five mice for AA group. Asterisks indicate statistically significant differences relative to the vehicle group, tested using one-way ANOVA followed by Dunnett's multiple comparisons test ($P = 0.030$ and 0.033, for 5-HT and AA groups respectively). (f) Intra-urethral stimulation with 5-HT (1 μM) and AA (1%) increases VMRs in response to intra-urethral distention (IUD). Area under the curve of VMRs elicited by IUD in mice perfused with intra-urethral saline (vehicle, open square symbols), 5-HT (1 μM; grey circle symbols) and AA (1%; blue circle symbols). Four mice are included in each group. Asterisks indicate statistically significant differences among the three experimental groups (V, AA, and 5-HT; one-way ANOVA Kruskal–Wallis test followed by Dunn's multiple comparisons test; $P = 0.02$ and 0.04 respectively).

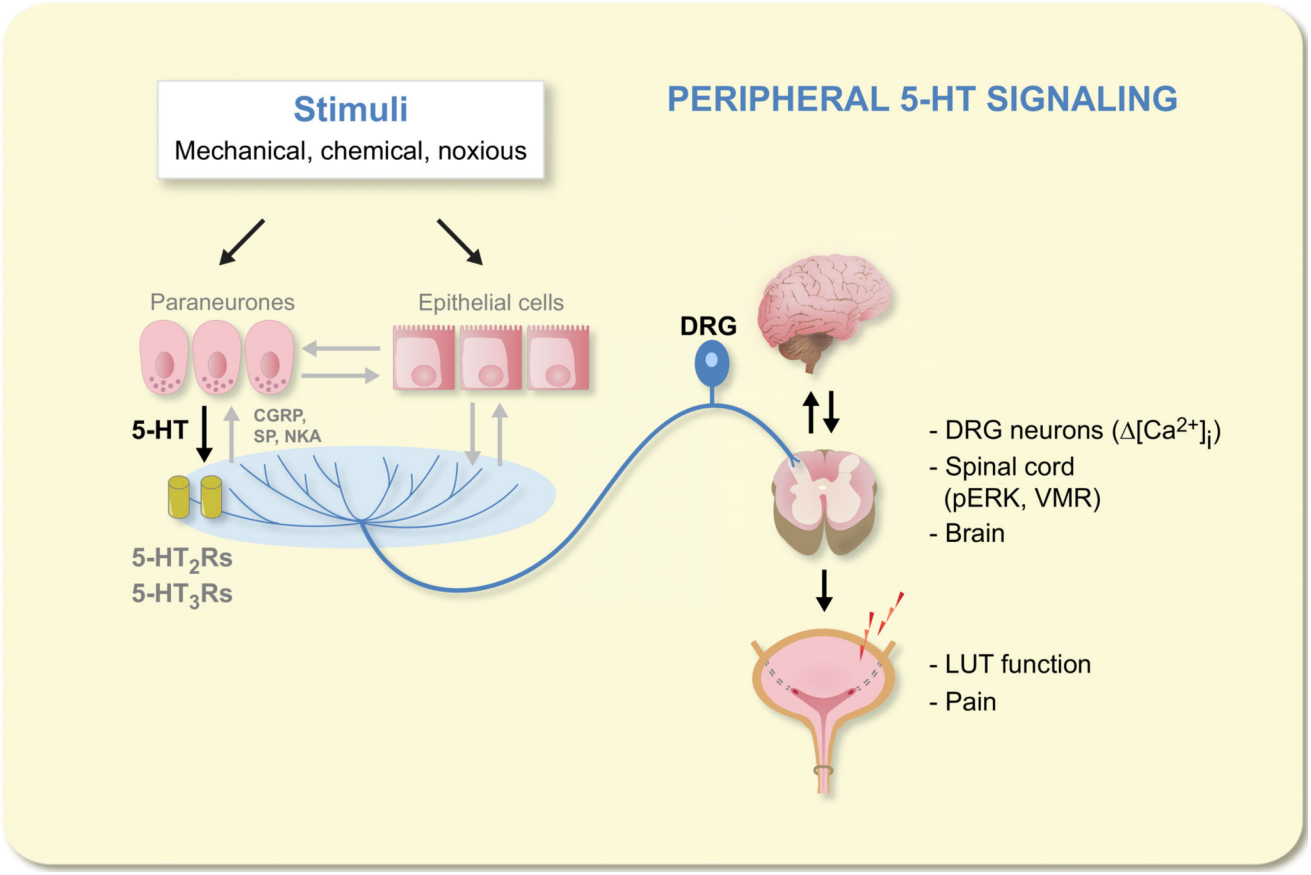

Figure 7.

Proposed diagram of peripheral 5-HT signalling. Various urethral stimuli (mechanical, chemical, noxious) reach the paraneurones and epithelial cells. In response, paraneurones release 5-HT that acts on 5-HT_2 and 5-HT_3 receptors on the afferent nerves (depicted in blue). Information is then transmitted to the dorsal root ganglia (DRG), spinal cord and brain and can influence lower urinary tract (LUT) function and pain/nociception. Additionally, 5-HT can act on epithelial cells that can in turn release transmitters to influence neuronal activity and paraneurones. The afferent nerves can also release peptides, CGRP, SP or NKA, to activate paraneurones and/or epithelial cells.

Table 1

Relationship between 5-HT$^+$ cells and nerve fibres in the urethra

Nerves	Markers	Relationship to 5-HT$^+$ cells
Sensory (C, Aδ fibres)	CGRP	Close proximity and possible contacts
Sensory (C, Aδ fibres)	SP	Close proximity and possible contacts
Sensory TRPV1 fibres	TRPV1	Close proximity and possible contacts
Efferent parasympathetic	nNOS, VAChT	No relationship
Efferent sympathetic	TH	No relationship

Each type of staining was performed in three to six mice.

Table 2

Primary antibodies used in this study

Marker	Target	Abs: host, purification method and catalog # (polyclonal or mc if indicated)	RRIDs AB Registry ID	Concentration
Serotonin (5-HT)[76]	Serotonergic cells	Goat, serum, Immunostar 20079	AB_572262	1 : 2500
		Rabbit, serum, Immunostar 20080	AB_572263	
Protein gene product 9.5 (PGP9.5)[77]	Neuronal marker	Rabbit, serum, Millipore, AB5925	AB_11214054	1 : 500
Cytokeratin 17 (CK17)[75]	Epithelial marker	Rabbit, immunogen affinity purified, Abcam AB53707	AB_869865	1 : 500
Calcitonin gene-related peptide (CGRP)[78]	Sensory C, Aδ fibres	Rabbit, serum, Sigma-Aldrich C8198	AB_259091	1 : 1000
Substance P (SP)[76]	Sensory C, Aδ fibres	Rabbit, whole serum, Immunostar 20064	AB_572266	1 : 1000
TRPV1 (VR1 N-Terminus)[79]	Sensory C-fibres	Rabbit, whole serum, Neuromics RA10110	AB_2208998	1 : 500
Synapsin I[80]	Presynaptic marker	Rabbit, immunogen affinity purified, Abcam ab8	AB_2200097	1 : 500
Neuronal nitric oxide synthase (nNOS)[81]	Efferent PSYM	Rabbit, Life Technologies 617000	AB_2533937	1 : 1000
VAChT[82]	Efferent PSYM	Rabbit, whole serum, Immunostar 24286	AB_572269	1 : 1000
Tyrosine hydroxylase (TH)[83]	Efferent SYM	Rabbit, Protein A purified, Abcam ab112	AB_297840	1 : 1000
pERK[46]	Phospho-p44/42 MAPK (Erk1/2) (Thr202/Tyr204)	Rabbit mc, Cell Signaling #4370	AB_10234795	1 : 1000
Tuj 1 (Neurone-specific class III beta-tubulin)[84]	Neurones	Chicken, affinity purified, Neuromics CH23005	AB_2210684	1 : 1000

RRID AB registry ID refers to the NIH Resource Identification Portal database for authentication of key biological resources (antibodies). References from previous studies using these antibodies are included. PSYM, Parasympathetic; SYM, Sympathetic.